



Epithermal activity in brecciated Permian-Triassic? arkose: a novel occurrence for the region at Los Cuatro Pozos quarry, southeastern San Luis province, Argentina

Raúl LIRA¹, Nicolás A. VIÑAS² and Héctor MAFFRAND³

¹Museo de Mineralogía y Geología "Dr. Alfred W. Stelzner" – Facultad de Ciencias Exactas, Físicas y Naturales – Universidad Nacional de Córdoba. CONICET. Av. Vélez Sarsfield 249, X5000JJC, Córdoba, Argentina.

²Michelotti e Hijos S.A., Sargento Cabral 916, 5151, La Calera, Córdoba, Argentina.

³Minería y Servicios S.A., Sargento Cabral 916, 5151, La Calera, Córdoba, Argentina.

Emails: n_vinas@michelotti.com; hmaffrand@yahoo.com

Editor: Anabel Gómez y Jorge Coniglio

Recibido: 10 de diciembre de 2023

Aceptado: 15 de marzo de 2024

ABSTRACT

Los Cuatro Pozos is an outcrop of silicified arkosic sandstones with fanglomerate levels, of continental origin and of probable Permian-Triassic age. A vertical fault zone crosscuts the quarry at least along 150 m with NE (25°) strike and a variable thickness of 5 to 10 m. In its SW edge, crackle-, mosaic-, and chaotic breccia types have formed, cemented by manganese oxides (hollandite), chalcidony, idiomorphic quartz and several generations of calcite. Anomalous contents of Ba in positive correlation with Mn, mimic the composition of Sr-rich hollandite. Anomalous geochemical values of Cu support the finding of supergenic Cu phases. Weakly anomalous Mo, V and Li are also registered. The positive correlation of Cu and V with Mn suggests its affinity with Mn oxides; however, the occurrence of Li and Mo is aleatory. The Co + Ni vs. As + Cu + Mo + Pb + V + Zn binary ratios support a hydrothermal origin for the Mn oxides. The trapping temperatures range of primary fluid inclusions in calcite (~ 192 to ~ 255 °C) suggests epithermal conditions. The presence of Tl adsorbed onto the Mn oxides, together with Cu, might be pathfinders of the existence of sulfides at depth. The epithermal event and the source of the fluids could be framed within a rift-related basin tectonic context, assuming the potential existence of underlying subvolcanic intrusives. A metallogenetic link with the magmatism of the Permian-Triassic Intracratonic Magmatic Corridor of La Pampa province is unlikely, considering that this one is located more than 120 km to the south.

Keywords: Extensional fault breccia, Mn oxides, carbonates, thallium, polymetallic anomalies.

RESUMEN

Actividad epitermal en arcosa ¿permo-triásica? brechada: un caso novedoso para la región en la cantera Los Cuatro Pozos, sudeste de la provincia de San Luis, Argentina.

Los Cuatro Pozos es un afloramiento de areniscas arcósicas silicificadas con niveles fanglomerádicos, de origen continental y de probable edad permo-triásica. Una zona de falla vertical atraviesa la cantera con rumbo NE (25°), en una extensión mínima de ~150 m con un espesor variable de ~ 5 a 10 m. En el extremo SO se han formado brechas de craquelación, en mosaico y caóticas, cementadas por óxidos de manganeso (hollandita), calcedonia, cuarzo idiomorfo y varias generaciones de calcita. Valores anómalos de Ba en correlación positiva con Mn, responden a la composición de la hollandita portadora de Sr. Valores geoquímicos anómalos de Cu respaldan el hallazgo de fases de Cu supergénicas. También se manifiestan contenidos levemente anómalos de Mo, V y Li. La correlación positiva de Cu y V con Mn sugiere su afinidad con los óxidos de Mn; sin embargo, la presencia de Li y Mo es aleatoria. Las relaciones binarias de Co + Ni vs. As + Cu + Mo + Pb + V + Zn, apoyan el origen hidrotermal de los óxidos de Mn. El rango de las temperaturas de entrapamiento de inclusiones fluidas primarias en calcita (~ 192 a ~ 255 °C) sugiere condiciones epitermales. La presencia de Tl adsorbido en los óxidos de Mn, junto al Cu, podrían ser indicadores de la existencia de sulfuros en profundidad. El

evento epitermal y la fuente de los fluidos podría enmarcarse en un contexto de tectónica de cuenca tipo rift, asumiendo la potencial existencia de intrusivos subvolcánicos subyacentes. Un vínculo metalogenético con el magmatismo del Corredor Magmático Intracratónico Pérmico-Triásico de la provincia de La Pampa es menos probable, considerando que éste se sitúa a más de 120 km al sur..

Palabras clave: Brecha de falla extensional, óxidos de Mn, carbonatos, talio, anomalías polimetálicas.

INTRODUCTION

The Los Cuatro Pozos sandstone quarry is located at 35°33'43''S and 65°10'03''O, ~ 22.3 km NE of Arizona locality (Dupuy Department), in the southeastern corner of San Luis province, near the border with La Pampa province (Fig. 1a-b).

Bulk rock mining of sandstone started systematically in 2004 by the company Minería y Servicios S.A., and has been active since then with sporadic interruptions due to market fluctuation. The total production up to date is ~ 800.000 Tn of crushed/sieved silicified arkose, mainly of 0/6 and 6/20 grain size, which is under norms suitable for asphalt mixtures, soil

stabilizing, ballast, breakwater and concrete. Petrographic and rock mechanic properties were determined to characterize its mineral composition and physical behavior (Viñas 2005). Currently, the quarry is being exploited along a west to east, ~ 50 m wide and 12 m high front at the topographic surface (Fig. 2). The actual depth in its second exploitation front is ~ 21 m. During early open-pit work (2004), the first bench exposed weak Mn oxides and carbonate veining which gradually increase in volume toward depth (second bench), with better exposures of a locally cemented brecciated sandstone. The main goal of this contribution is to provide evidence of the existence of a partially mineralized linear breccia that crosscuts the arkose

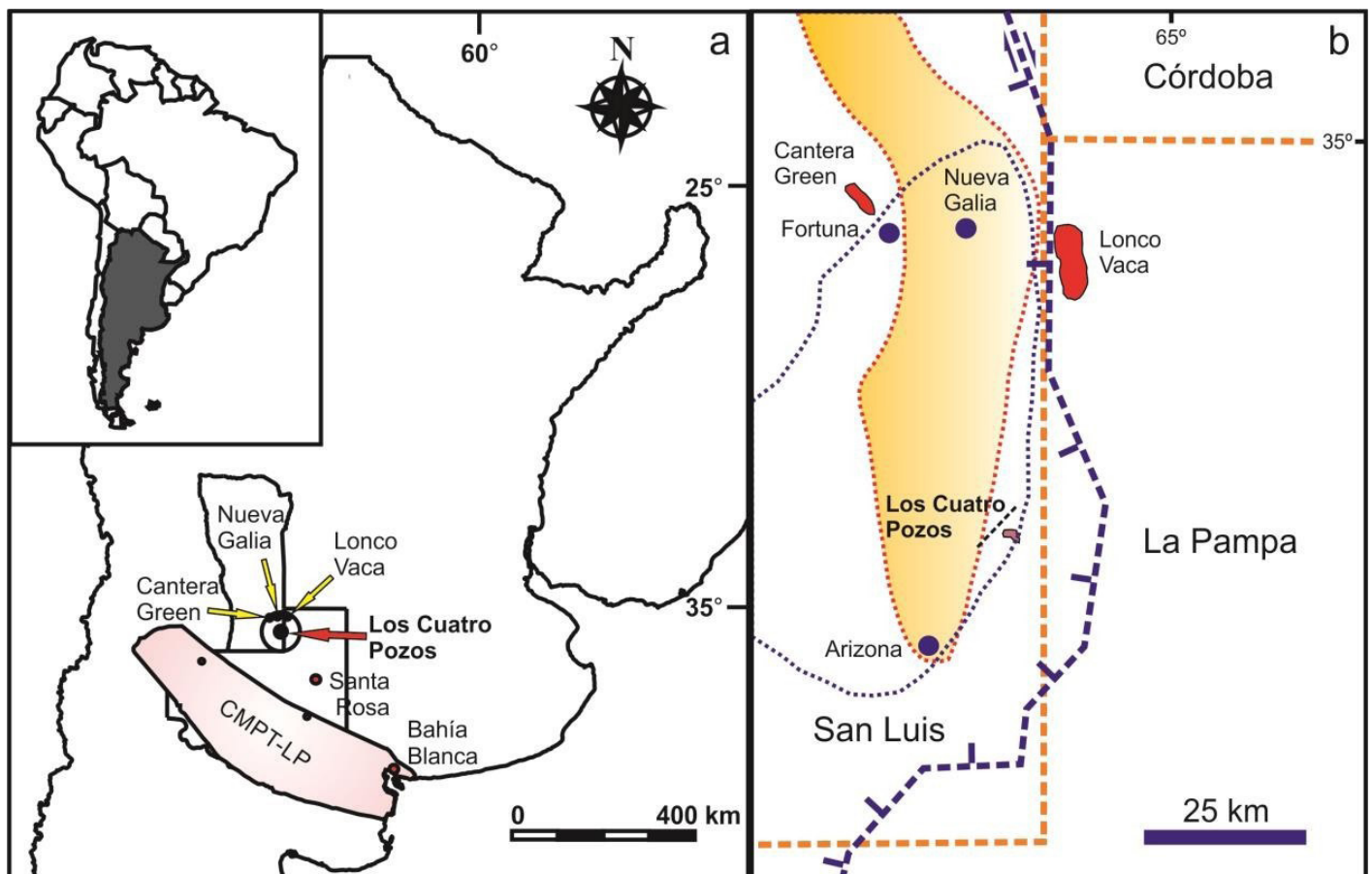


Figure 1. a. Location map of the Los Cuatro Pozos sandstone quarry in southeastern San Luis province. The Permian-Triassic Magmatic Corridor of La Pampa province (CMPT-LP, Chernicoff et al. 2019) is drawn to show the nearest outcropping evidence of magmatic (and epithermal) activity in the neighboring region. b. The Nueva Galicia basin (shaded area) and neighboring Pampean basement outcrops (Lonco Vaca and Green quarries) were added for reference (modified from Kostadinoff et al. 2006). The dashed line at NW of the arkose outcrop is a fault mapped by de Elorriaga and Tulio (1998) which is indicated in situ by a NE-SW channelled terrain depression of ~ 40 m deep below the plain's surface. The contoured dotted line is part of the Arizona basin, limited to the east by a large-scale transtensional fault (dashed line with indication of the downward block) active during the Upper Devonian, according to Chernicoff and Zappettini (2007).

outcrop. Field, mineralogical, petrographic, geochemical and preliminary fluid inclusion microthermometry studies demonstrate the epithermal origin of the mineralizing fluids, which would have circulated along extensional structures of late or post-Permian-Triassic age.

Regional and local geology: Previous work

Based on earlier drill hole and refraction seismic data, de Elorriaga and Tullio (1998) studied the behavior of the different geological formations and of the basement at depth in relationship with the relief and lineaments, in the northern region of La Pampa province, including the southeastern portion of San Luis. In this area they mapped a fault trace of NE strike located at ~ 5 km west of the Los Cuatro Pozos quarry; this fault would be indicated by a NE-SW topographic depression of ~ 40 m below the plain level (Fig. 1b). De Elorriaga and Tullio (1998) described the representative sedimentary outcrops of the Los Cuatro Pozos quarry as a sequence of banks of immature material of variable grain size, earlier classified as arkose by Romero (1960). It consists of an undeformed com-

act hard rock (at microscopic scale), tentatively assigned to the Paleozoic and without geological correlation with other lithological formations of the region (de Elorriaga and Tullio 1998). Kostadinoff et al. (2006) conducted geophysical surveys (gravimetric, magnetometric, density and magnetic susceptibility studies) in the southern region of San Luis province, to elaborate a geological model of the area, including the Los Cuatro Pozos quarry. These authors described the sandstone outcrops as slightly folded. According to de Elorriaga and Tullio (1998), sandstones of similar characteristics crop out southeast of Los Cuatro Pozos at Ea. Alto Verde (Fig. 1a).

The Nueva Galia-Arizona basin, defined by a gravimetric survey (narrow and extensively developed in length) was interpreted as a rift type basin (Fig. 1b). The northern area of this rift basin is bounded by basement rocks that crop out in the Lonco Vaca and Green quarries. At the Green quarry (NW of Fortuna), the representative rocks are foliated granites with K-feldspar megacrysts and micaceous schists intruded by pegmatite and granite dikes. These basement rocks are correlated with those cropping out at Lonco Vaca, where the main



Figure 2. Google Earth satellite image of the Cuatro Pozos sandstone open pit, camp and bulk-rock processing plant (Minería y Servicios S.A.). The original boundary of the sandstone outcrop, prior to mining, is approximately outlined. The actual depth is approximately 21 m. Overburden is a loess-like sediment of variable thickness (up to 1 m) topped with soil, with localized calcrete layers (up to 40 cm thick). The trace of the fault breccia is sketched.

rocks are amphibolites, micaceous schists, gneises and foliated granites intruded by pegmatite and granite dikes. These metamorphic-igneous deformed rocks were assigned to the Pampean Orogeny (Neoproterozoic-Lower Cambrian), likely as a southern extension of the Comechingones and Yulito ranges (Linares et al. 1980, Kostadinoff et al. 2006), whereas the non-deformed granitoid rocks were assigned by Parica (1986) to different intrusive events extended from Precambrian to Carbonic times. Regarding the sedimentary features of the basin infill sedimentation, Kostadinoff et al. (2006) suggested that the only available evidence that can be used to infer its composition are precisely the Los Cuatro Pozos arkosic sandstones located in the southeastern border of the basin delineated boundary. The authors described the arkose of Los Cuatro Pozos as grey-purple, weakly folded rocks striking 270° and 0° with low dips (35° - 5°) to the N, NE and E, with a porosity of up to 20 %. Kostadinoff et al. (2006) described alternating coarse and fine grained banks, sometimes decreasing grain size sequences up to 5 m thick that may finish up in thin levels (< 5 cm thick) of red mudstones, which may show ripple-marks. Infrequent cross-bedded structures are restricted to sandy levels. Their mineralogical and textural descriptions of the arkose generally agree with the petrographic descriptions of de Elorriaga and Tullio (1998) and with our own studies. Among the scarcely present minerals, Kostadinoff et al. (2006) mention epidote and zircon; they recognized oxidation and Fe-loss of biotite booklets and the formation of spotty concentrations of Fe-oxide-hydroxide associated to the finer clastic fraction. According to Kostadinoff et al. (2006), neither pegmatite clasts nor clastic granite/pegmatite minerals show inherited ductile deformation. They classify the rocks as arkosic arenites, fanglomerates and breccias. The sedimentation environment is assigned to proximal alluvial fans, related to basin borders associated with extensional faulting. The authors assume that at least part of the Nueva Galia basin infill could be sedimentites similar to those of the Los Cuatro Pozos outcrop.

According to de Elorriaga and Tullio (1998), the Los Cuatro Pozos sandstones are equivalent to the Arata Formation, assigned by Salso (1966) to the Permian-Triassic period. The pegmatite and micaschist clastic fraction found at Los Cuatro Pozos is very similar to the lithologies recognized in Sierra de Lonco Vaca (Fig. 1b, Párica 1986, Kostadinoff et al. 2006). Kostadinoff et al. (2006) interpreted that the metamorphic rocks of Pampean ages were part of the oriental basement border of the Nueva Galia basin. The ages of several intrusive events determined by Párica (1986) at Lonco Vaca cover the Precambrian-Carboniferous time span. The infill of the Nueva Galia basin might have started during the Upper Carbonifer-

ous and extended to the Mid-Upper Triassic, as it occurred in the neighboring Alvear basin (Kostadinoff et al. 2006).

From a geotectonic perspective, based on field and gravimetric data, Chernicoff and Zappettini (2005a, 2005b, 2007) considered the Los Cuatro Pozos outcrop as part of a larger neopaleozoic transtensional pull-apart basin named Arizona basin, which was interpreted as the southern extension of the Paganzo basin (Fig. 1b). The same authors also identified two other smaller depocenters north-south aligned with the Arizona basin, located in the central-northern area of La Pampa province, named Telén and Daza; these depocenters are related to gravimetric lows as also were considered others aligned in a N-S direction located in northern San Luis province (i.e., Bajo de Véliz), and northwestern Córdoba province (i.e., Chancaní and Tasa Cuna). The origin of the Arizona basin and related N-S aligned depocenters would have been controlled by the Chanic deformation phase during the Upper Devonian that reactivated the Lonco Vaca - Valle Daza fault (Chernicoff and Zappettini 2007).

LOCAL GEOLOGY

The study area, except for the isolated outcrops affected by the quarry exploitation, is covered by farming soils that developed over quaternary alluvial plains and old distal alluvial fans (Costa et al. 1999), previously described as dune plains (González Díaz 1981).

Our field observations largely agree with information provided by previous researchers. Nevertheless, we provide new geologic data available due to the quarry exploitation, particularly focused in the surroundings of a partially brecciated fault zone.

The Los Cuatro Pozos quarry crops out in an area of ~ 8 ha, about 20 m above the surrounding plain level (Fig. 2); overburden of variable thickness (0.3 up 2.5 m) is composed of loess-like sediments and soil cover (Fig. 3). The uplift of Los Cuatro Pozos arkose was interpreted by de Elorriaga and Tullio (1998) as the result of differential tectonics controlled by reverse-reactivated faults, which led to SW to NE small elongated blocks limited by two fracture systems: NW-SE, interpreted as probable faults, and NE-SO, mapped as identified faults. The dominant rock is largely arkose though interbedded fanglomerate lenses do occur with erratic distribution. An extensional fault zone ~ 5 to 10 m thick crosscuts the sandstone along a 25° NE strike along 150 m (maximum extension along fault exposed by mining works; figures 2 and 3). Several parts of the fault expose monomictic breccias, cemented by different pulses of calcite, manganese oxides and



Figure 3. View of the SW margin of the quarry. The wavy dotted (yellow) line shows the contact between the arkose and overlying regolith and loess-like sediments and soil cover. Black stains are Mn oxides that roughly delineate the SW edge of the fault breccia zone; however, the image view is oblique to the strike of the fault zone/breccia, hence what is shown is the width along the bench and not the thickness of the brecciated-mineralized lineament which is 5 to 10 m. The arrow points at a breccia body (between red-dashed lines) shown in detail in figure 5.

silica, particularly in its SW edge (Fig. 5); in its NE quarry edge the cementation by Mn oxides and carbonates is less intense and localized (Fig. 6). The strike of this fault (25°) is within the NE-SW strike range assigned by de Elorriaga and Tullio (1998) to a fault mapped about 5 km NW of the Los Cuatro Pozos quarry. This fault trace is indicated in the terrain by a longitudinal depression of ~ 40 m deep with respect to the surrounding plains, which shifts its strike more to the south, southwest of the quarry location. The strike of this fault looks similar to the structural design observable at Lonco Vaca, east of Nueva Gallia (de Elorriaga and Tullio 1998).

Breccia description

The brecciated sandstone shows transitions from mosaic to chaotic breccias, and locally to crackle-breccias (Fig. 7a-b). The fragments are sharp angular, varying in size from ~ 30 cm in the largest blocks down to several millimeters sized chips; rock-flour is absent. Breccias are clast- to subordinate matrix-supported. Several centimeters sized open voids are present though most are filled with calcite \gg Mn oxides. Banded and drussic textures are commonly developed by cementing manganese oxides, subordinately followed by chalcedony, idiomorphic drussic quartz, and by several generations of calcite (Cc1 to Cc4; Fig. 8a-b-c-d). A distinct generation of fine-grained quartz (botryoidal chalcedony) sporadically occurs elsewhere in the quarry as light bluish to grey thin coatings or patches in fractures, or rimming cavities from 0.1 mm to sev-

eral centimeters long; its origin could not be paragenetically related to any of the other identified silica pulses. The crystallization sequence of breccia cementing phases (Mn oxides, silica and carbonates) in relationship with early diagenetic silicification processes (Cd1, Qz1 and Opl, as abbreviations for chalcedony, quartz and opal, respectively) and supergene redistribution is depicted in figure 9.

Mn oxides (largely hollandite, see below; Fig. 8) were the first precipitating phase in the breccia zone (Hol1). These oxides occur as thin coatings less than 0.5 mm thick; only one main pulse was identified though it sporadically deposited after the second generation of Cc2- calcite (Hol2). Chalcedony bands less than 2 mm thick (Cd2) deposited after Mn oxides and prior to earliest calcite (Cc1). Mn oxides crystallized over chalcedony were not observed. Calcite crystallized after Mn oxides or after chalcedony where the latter was present. At least five different pulses of calcite deposition were identified (Cc1 to Cc5). Zonation of calcite bands may have also deposited directly on the sandstone as breccia cement. Thicknesses of each pulse vary, ranging from a few millimeters up to 4 cm. The different zones may vary in color from pale beige to white; some of the growth bands offer pale yellow fluorescence, under long UV wavelength alternating with non-fluorescent bands (Cc1 to Cc4). One of the intermediate pulses that formed druse-lining rhombohedral crystals fluoresces under short UV wavelength in moderately strong yellowish green color. In some voids, a second generation of idiomorphic

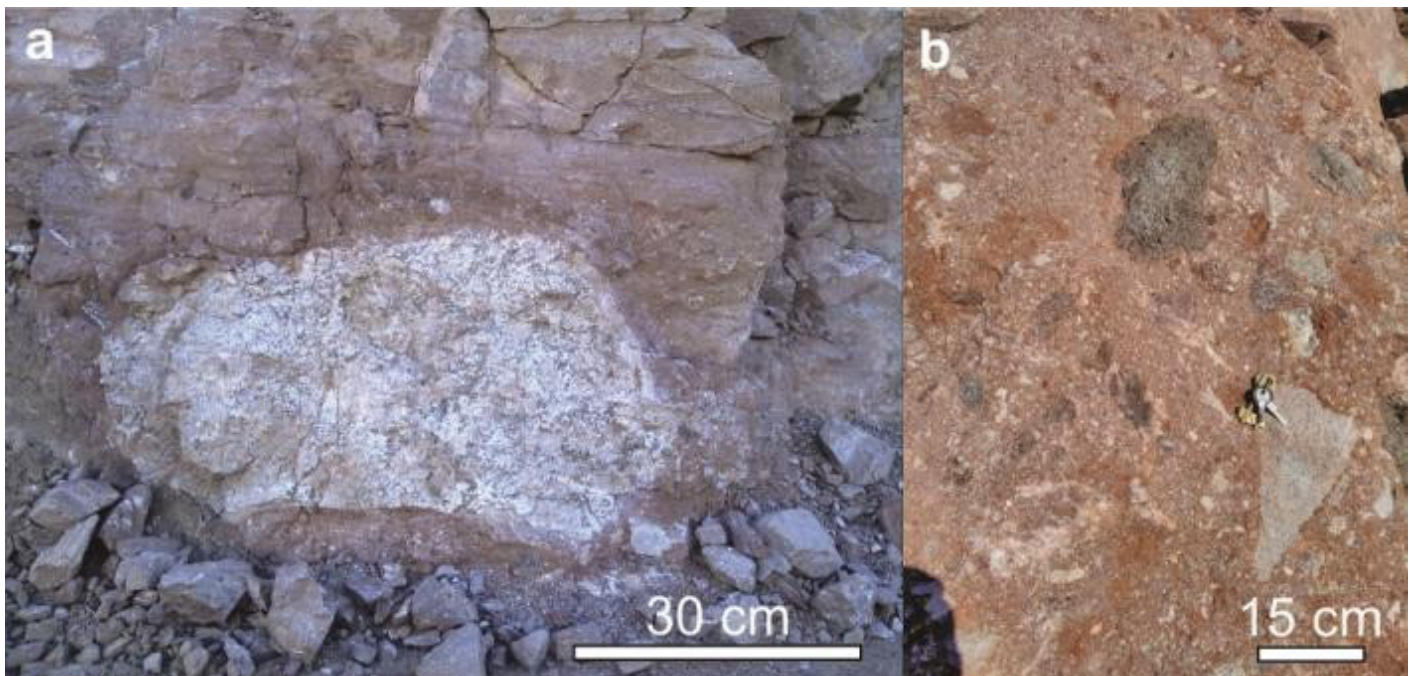


Figure 4. a. Subhorizontal arkose strata with a large, partially argillitized coarse-grained to pegmatitic granite block within a flanglomerate lense (bottom of 2nd level, south verge). b. Flanglomerate lense with variable sized clastic fractions of weathered schists and granitoid rocks.

quartz (Qz2) has crystallized over chalcedony (Cd2) rimming drussic cavities; also, a third generation of chalcedony and idiomorphic quartz (Cd3 and Qz3) can be sporadically found over Cc2 carbonates. The latest phase deposited in voids is scalenohedral calcite (Cc5). Mn oxides, silica and carbonate phases all may be found as independent veinlets hosted in the brecciated arkose; these only occur associated in successive paragenetic sequences in the largest cavities or broadest fractures. We have not found any evidence of arkose alteration within the breccia zone (i.e., pervasive alteration of the breccia clasts), neither outside the fault breccia.

ANALYTICAL METHODS

Five thin section petrographic analyses by optical refraction/reflection microscopy were performed on representative sandstone and brecciated-mineralized sandstone samples. X-Ray diffraction (XRD) analyses were applied to two representative hand-picked samples of Mn oxides for species identification. Both powdered samples were run in a Phillips PANalytical XPERT-PRO diffractometer operating with a Cu anode, under a continuous scanning mode from 7 to 70° and 0.026 two theta of step size (generator setting: 40 kV and 40 mA); XRD data were acquired at the INFIQC, Facultad de Ciencias Químicas (National University of Córdoba, Argentina). Polished thick sections of Mn oxides aggregates were analyzed through energy dispersive spectrometry (EDS) coupled with

a Carl Zeiss FE SEM SIGMA scanning electron microscope (SEM), located at the Laboratorio de Microscopía Electrónica y Análisis por Rayos X (LAMARX), Facultad de Matemáticas, Astronomía, Física y Computación (National University of Córdoba). Two bulk-rock exploration samples from the brecciated mineralized zone (Mn1: Mn oxide rich, MnCalc2: calcite-rich + Mn oxides), one representative non-mineralized arkose sample (Ark) outside the breccia zone, a hand-picked purified Mn oxide concentrate (4Pz-1) and a composite sample made up of two different closely located sampling spots (4Pz-1-2), were analyzed in the laboratories of Alex Stewart International Argentina S.A., using their commercial analytical package ICP-MA-42 (42 elements). The methodology consisted in dissolution of 0.2 g of pulverized sample in four acids (total digestion in hydrofluoric, perchloric, nitric and hydrochloric mixed acids (partial loss of As, Cr, Sb and Hg through volatilization), and element concentration determination by Radial ICP-OES. A fifth composite sample (4Pz-1-4Pz-2) was tested for Au using their commercial Au4-30 package, in which Au is analyzed in 30 g of sample by fire assay and measured by atomic absorption spectroscopy (see analytical results and instrumental detection limits in table 1). Heating runs were done in a FLUID INC stage set up at the CNEA (National Atomic Energy Commission, Regional Centro, Córdoba, Argentina); the thermal working range of the equipment is - 196 °C to + 700 °C (± 0.1 °C precision between - 56.6 °C and + 660.4 °C). The mineral abbreviations are from Warr (2021) after the IMA-CNMNC approved list.



Figure 5. Vertical breccia body at the SW edge of the quarry (see location in figure 3). Chaotic-, locally collapse- monomictic arkose breccia cemented by Mn oxides (black stains) and various pulses of calcite (white stains). Double pointed red arrows are parallel to stratification, which is almost horizontal outside the breccia body and randomly oriented in the clastic fragments within the breccia body.

RESULTS

Arkose petrographic description

The representative sandstone is a reddish purple strongly coherent rock formed by a dominant angular to subangular clastic fraction (80-85 %), composed of quartz (~ 49 %) feldspars (~ 25 %; K-feldspar >> plagioclase), lithic fragments (~ 7 %) and muscovite and biotite (~ 3 %) in a finer grained matrix (15-20 %). About 3 % volume of the matrix are cavities partially or completely filled in with silica minerals. Elongated

clasts are normally aligned indicating stratification planes.

The grain size of the clasts is bimodal, with the coarse grained fraction prevailing over the finer grained one. The largest clasts (0.5 mm average, rarely up to 2 mm) are angular to subangular lithic fragments largely of muscovite-biotite granite or clasts of granitic minerals (quartz, K-feldspar, plagioclase, muscovite and biotite). Most of the largest quartz and feldspar clasts show undulose extinction indicative of inherited deformation. The finer fraction (average size ~ 0.1 mm) is composed of sub-rounded to rounded clasts. Clastic quartz



Figure 6. Fault zone (multidirectional fracturing) at the NNE edge of the quarry where cementation is weaker and localized; right-pointing arrows indicate Mn oxides whereas the arrow pointing to the left shows calcite veining.

occurs as individual grains or as mosaic aggregates with sutured intergranular contacts. Microcline shows well-developed tartan twinning and is slightly altered to phyllosilicates. Plagioclase shows the typical polysynthetic albite twinning, some with wedge shaped and bent or displaced lamellae; some crystals are zoned with a more calcic core differentially altered to sericite and clay minerals. Inclusion-free, non-phenogitic muscovite clasts (125 - 650 μm) occur in tabular sheet aggregates, in some cases deformed and shredded. Biotite sheets (~ 500 μm) are scarcer than muscovite and frequently replaced by muscovite with cleavage-hosted secondary Fe-Ti-oxides.

The matrix fraction is composed of finer-grained clasts of the same composition as the coarser fraction (between 20 and 150 μm) plus fluorapatite and zircon with Fe-oxides/hydroxides impregnations along intergranular contacts.

The cement is composed of crystalline, microcrystalline and amorphous silica, i.e., quartz>chalcedony>>opal (Fig. 10a-b). Quartz precipitated as tiny idiomorphic prismatic crystals of radiating habit with growth zonation, rimming sedimentary clasts. Chalcedony and opal typically fill small voids. The depositional sequence of cementing silica phases is typically quartz→chalcedony→opal (Fig. 9). Due to silica cementation, the Los Cuatro Pozos arkose is a strongly coherent rock, a fact that likely favored its positive topographic exposure above the surrounding plains. In this regard, the Los Angeles test was used to measure the resistance to fragmentation and abrasion of coarse-grained crushed arkose aggregates, which yielded values of 24.7 and 26.1 %, respectively (Laboratorio de Estructuras 2016, 2021).

Mn oxides mineralogy

Manganese oxides are irregularly distributed along the fault breccia in reduced volumes. Mn oxides either cement breccia clasts or are more commonly widespread as thin coatings on fractures, normally as powdery aggregates; massive veinlets are scarce and can hardly reach 5 mm thick. Secondary electron images (SEI) show aggregates of micrometric (< 5 μm) prismatic crystals (Fig. 11a). Energy dispersive spectrometry (EDS) analyses were performed in samples Mn1 and MnCalc2 on polished thick sections, which yielded the following average composition in weight % (N = 10) and ranges between brackets: MnO = 78.21 (74.75 - 82.39), BaO = 15.94 (12.60 - 20.62), SrO = 1.94 (0.00- 3.54), CaO = 1.33 (0.89 - 1.91), SiO₂ = 0.97 (0.00 - 2.03), K₂O = 0.64 (0.00 - 0.76), Na₂O = 1.46 (0.00 - 2.05) and Al₂O₃ = 0.90 (0.58 -1.37). Except for Mn and Ba, Sr and Ca are ubiquitous, except for one analytical spot each; K and Si were present in eight and



Figure 7. a-b. Brecciated arkose cemented by thin coatings of Mn oxides (largely hollandite) and several generations of calcite.

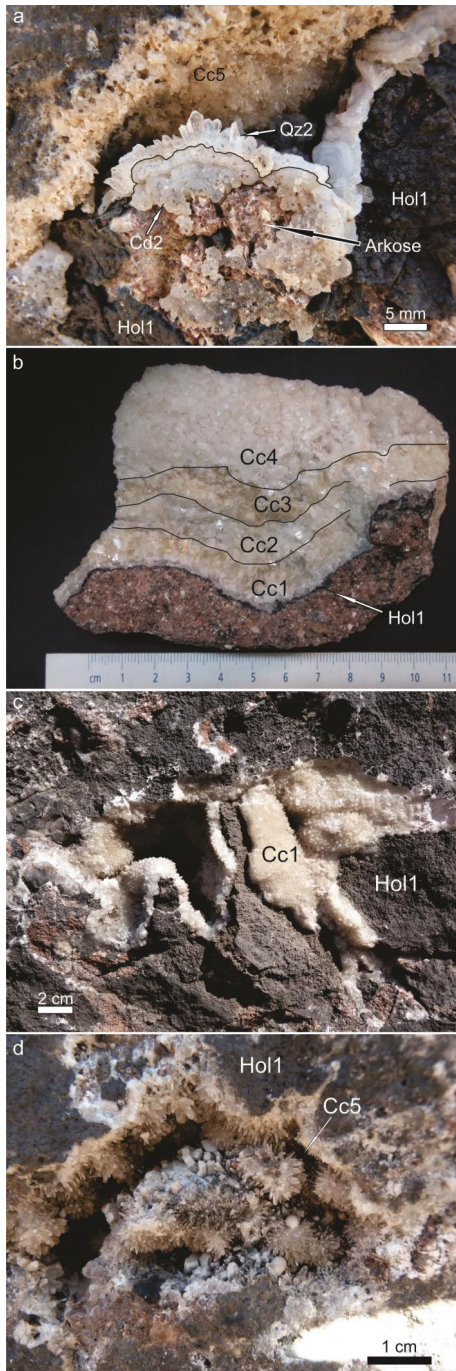


Figure 8. Representative textures of the SW edge of the breccia zone. a. Crystallization sequence in void started with Mn oxides (Hol1), followed by botryoidal chalcidony (Cd2), idiomorphic quartz crystals (Qz2) and late stage scalenohedral calcite (Cc5). b. Rhythmic deposition of several pulses of medium-sized grained calcite distinguished by color; the pale beige colored bands emit weak green yellowish fluorescence under long wave UV light. Calcite 1 (Cc1) precipitated over earlier hollandite (Hol1) but in other cases it deposited over chalcidony (Cd2). c. Rombohedral-terminated calcite filling druses over hollandite (Hol1), equivalent to one of the pulses Cc1 to Cc4; in some sectors a third generation of botryoidal chalcidony and idiomorphic quartz crystals (Cd3 and Qz3) might have crystallized over Cc1 or Cc2. d. The latest generation of calcite (Cc5) is represented by scalenohedral calcite (the thickest whitish prismatic-looking crystals lining vugs represent an early generation of truncated scalenohedrons).

six out of ten of the analyzed areal spots, respectively, whereas Al and Na were present in about half of the analyzed spots (Fig. 11b). Under reflected light (air), polished thick sections of samples Mn1 and MnCalc2 showed the same known optical properties published in the literature for hollandite. Two samples (Mn1 and 4Pz-1) were examined by XRD; due to its extremely fine grain size (sooty texture) and difficulties on getting pure hand-picking separates, both samples yielded contaminated patterns with minor quantities of quartz and K-feldspar, or calcite. A poor quality XRD pattern of sample Mn1 showed reflections of a non-identified Mn oxide phase mixed with quartz and calcite, whereas sample 4Pz-1 clearly evidenced the presence of hollandite $[\text{Ba}(\text{Mn}^{4+}_6\text{Mn}^{3+}_2)\text{O}_{16}]$. Its main twelve peaks (d in Å) and intensities (% between brackets) that match the pattern list of reference code # 00-034-0174 from the International Centre for Diffraction Data (ICDD), are the following: 3.143 (100), 3.101 (98), 2.412 (73), 3.178 (58), 3.069(58), 3.522(35), 3.460(35), 2.181(32), 2.153(29), 2.204(25), 2.173(24) and 1.822(24).

Whole-rock geochemistry

Two samples from the brecciated mineralized zone (Mn1 and MnCalc2), one representative non-mineralized arkose sample (Ark) outside the breccia, and a hand-picked purified Mn oxide concentrate (4Pz-1), were analyzed for major and trace elements. Composite Mn oxide-rich sample 4Pz-1-2 was analyzed only for gold. The obtained results are presented in table 1.

Mn1 sample represents part of the brecciated arkose sandstone cemented by Mn oxides with scarce or lack of visible carbonates, whereas MnCalc2 represents another zone of the breccia also mineralized with Mn oxides but with abundant carbonates in veinlets and as druse infilling. In both samples, the total content of Mn varies from ~ 0.7 to 1.87 wt. %. The Fe content is very low (< 1 wt. %) in both samples. No other significant variations were found in the whole rock chemistry of major elements. Both samples are notoriously enriched in Ba, which varies from 1652 ppm (Mn1) to more than 2000 ppm (above detection limits) in MnCalc2, indicative of a positive correlation of Ba with Mn, suggesting a possible hollandite (or romanéchite) "component" in the Mn oxides. None of the pathfinders of epithermal precious metal (Au, Ag) mineralization were detected in anomalous contents (e.g., As). Sample 4Pz-1-2 was analyzed for Au and yielded negative results (< 0.01 ppm) as well as for Ag in this and the other three mineralized samples. Copper shows an anomalous value in the Mn oxide bearing, carbonate-enriched sample (MnCalc2= 98 ppm) and it reaches its maximum content (592 ppm) in the hand-picked Mn oxide concentrate (sample 4Pz-1). Mo, V and Li are slight-

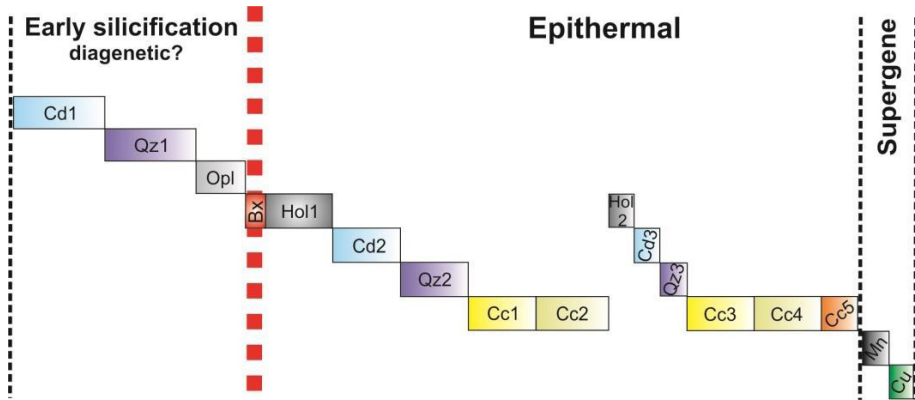


Figure 9. Early to late crystallization sequence of cementing phases at the Los Cuatro Pozos quarry. The earliest stage of massive silicification of arkose is interpreted as a diagenetic process as it affects the whole outcrop regardless of the fault zone. The vertical red dashed line represents the brecciation event (Bx). Cd: chalcidony, Qz: quartz, Opl: opal, Ho1: hollandite, Cc: calcite (darker yellow pulses are fluorescent), Mn: unidentified Mn oxides, Cu: secondary copper phase (likely chrysocolla).

ly anomalous only in sample MnCalc2 (24, 110, and 50 ppm, respectively). The Sr content is higher in the carbonate rich sample (Mn1 = 205 ppm and MnCalc2 = 660 ppm). The Mn oxide concentrate (sample 4Pz-1) analysis confirms a positive correlation between Ba and Mn. The highest Cu value (592 ppm) is also associated with highest Mn, Ni (48 ppm), V (400 ppm), Zn (112 ppm) and Sr (> 2000 ppm, above detection limit) values. Sample 4Pz-1 displays the lowest Li value (28 ppm), comparable to the non-mineralized arkose (34 ppm). A remarkable feature of the Mn oxide concentrate is the existence of anomalous contents of Tl (487 ppm), which is below detection limits (< 5 ppm) in all the remaining analyzed samples.

The non-mineralized arkose (Ark) sampled away from the breccia zone, without visible Mn oxides and carbonates, has an anomalous Ba content (434 ppm) though ~4 times less than the whole rock Ba content in the breccia zone; the abundance of K-feldspar and lithic fragments of granitic composition could account for these high Ba values. Total Fe in the non-mineralized arkose (Ark) is 1.09 wt. %, more than double the Fe content of the Mn oxide concentrate, suggesting that this is a representative Fe content for the sandstone. The Mn and Ca contents of the arkose are 0.06 and 0.32 wt. %, respectively, which look like representative values for the low Mn and Ca contents of the dominant granitic protolithic clastic fraction of the sandstone, as is evidenced by the high values of Al and K (K-feldspar rich).

Preliminary microthermometric data on hydrothermal calcite

Fluid inclusions in calcite are abundant, mostly aligned along prismatic and rhombohedral growth planes (Fig. 12a-b); however, most of fluid inclusions are monophasic, hence, measurable fluid inclusions are rather scarce. Heating runs were performed in seven isolated fluid inclusions, interpreted as of primary origin; all of these are anhedral to subhedral with

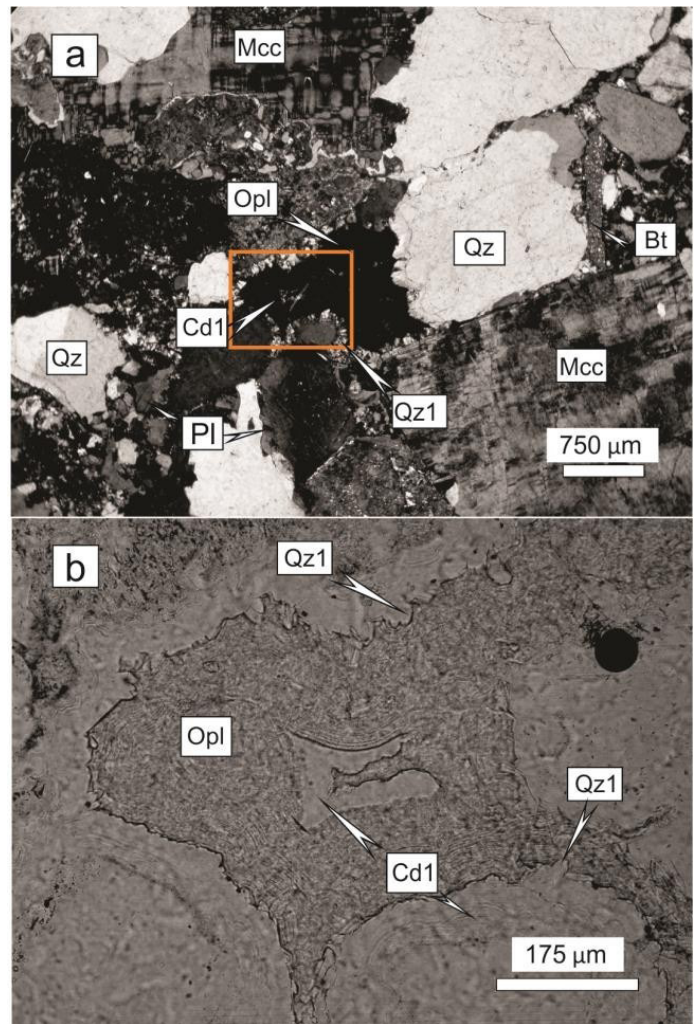


Figure 10. Thin section photomicrographies of representative silicified arkose. a- The framed area is enlarged in figure b, showing the silica phases responsible for the strong silicification of arkose. Abbreviations: Bt: biotite, Cd: chalcidony, Mcc: microcline, Opl: opal, Pl: plagioclase, Qz: quartz. Numbers following abbreviations refer to the crystallization sequence order, as established in figure 9.

irregular shapes and sizes ranging from 7 to 40 μm. Biphasic fluid inclusions are liquid-rich showing liquid/vapor ratios ranging from 0.7 to 0.9 (Fig. 12c). Homogenization temperatures

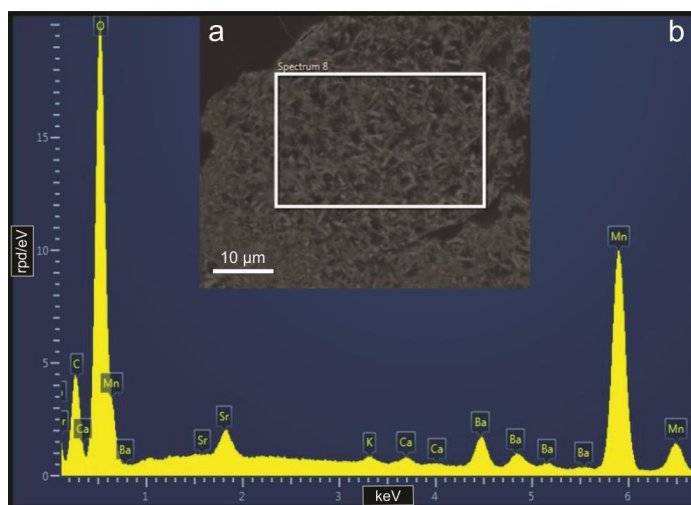


Figure 11. a. Secondary electron image (SEI) of intergrown hollandite crystals in polished thin section (Sample Mn1). b. Representative EDS compositional spectra of hollandite (Sample Mn1).

($n = 5$) to liquid range from 191.7 to 254.8 °C (average = 231 °C); at ~ 260 °C massive decrepitation of monophasic fluid inclusions starts and host calcite turns into a yellowish color. One large anhedral flat fluid inclusion (30 μm; $F = 0.85$) homogenized at 111.4 °C, but failed to renucleate the gas bubble upon cooling; this one and another that homogenized at 143.3 °C probably belong to the same population of likely secondary origin.

DISCUSSION

Origin of Mn oxides and other metals

The metal ratios used by Nicholson (1992) i.e., $Co + Ni$ vs. $As + Cu + Mo + Pb + V + Zn$ were applied to discriminate between hydrothermal and supergene Mn oxides; the results show that the analyzed samples plot within the hydrothermal field (Fig. 13). The X-ray diffraction analyses and EDS results indicate that the main Mn phase as breccia cement is hollandite. Even though hollandite was pointed out by Nicholson (1992) as one of the several Mn phases of preferential supergene origin (versus those of typical hydrothermal genesis), the hollandite occurrence at the Los Cuatro Pozos quarry is confined to the fault breccia lineament, where it texturally represents the earliest precipitated phase of a crystallization sequence that reached temperatures up to 255°C in later calcite; additionally, its microcrystalline texture does not show any evidence of a supergene replacement origin after an earlier phase.

The positive correlation between Cu and Mn suggests a genetic link between Cu and Mn oxides. The presence of a scarce light bluish unidentified discrete secondary Cu phase (likely chrysocolla) of erratic distribution (Fig. 14), interpreted

Table 1. Whole-rock geochemical analyses.

		Ark	Mn1	MnCalc2	4PZ-1	4PZ-1-2
Au	ppm	n.a.	n.a.	n.a.	n.a.	< 0.01
Ag	ppm	<0.5	<0.5	<0.5	<0.5	n.a.
Al	%	4.68	4.56	3.78	3.33	n.a.
As	ppm	9	<5	14	7	n.a.
Ba	ppm	434	1652	>2000	>2000	n.a.
Bi	ppm	<5	<5	<5	<5	n.a.
Ca	%	0.32	3.93	9.03	0.72	n.a.
Cd	ppm	<1	<1	<1	1	n.a.
Ce	ppm	45	38	29	49	n.a.
Co	ppm	2	5	11	29	n.a.
Cr	ppm	9	14	10	8	n.a.
Cu	ppm	14	34	98	592	n.a.
Fe	%	1.09	0.85	0.69	0.44	n.a.
Ga	ppm	15	13	12	10	n.a.
Hg	ppm	<2	<2	<2	<2	n.a.
K	%	4.13	3.83	3.17	3.33	n.a.
La	ppm	24	24	30	134	n.a.
Li	ppm	34	32	50	28	n.a.
Mg	%	0.1	0.11	0.14	0.23	n.a.
Mn	ppm	595	6708	18697	>20000	n.a.
Mo	ppm	<1	8	24	<1	n.a.
Na	%	1.15	0.8	0.6	0.59	n.a.
Nb	ppm	9	5	4	<1	n.a.
Ni	ppm	4	5	8	48	n.a.
P	ppm	609	708	769	312	n.a.
Pb	ppm	19	23	23	31	n.a.
S	%	<0.01	<0.01	<0.01	0.02	n.a.
Sb	ppm	<5	<5	<5	<5	n.a.
Sc	ppm	<5	<5	<5	<5	n.a.
Se	ppm	<10	<10	<10	<10	n.a.
Sn	ppm	<20	20	<20	<20	n.a.
Sr	ppm	64	205	660	>2000	n.a.
Ta	ppm	<10	<10	<10	<10	n.a.
Te	ppm	<10	<10	<10	<10	n.a.
Th	ppm	<10	18	15	<10	n.a.
Ti	%	0.07	0.07	0.07	0.05	n.a.
Tl	ppm	<5	<5	<5	487	n.a.
U	ppm	<10	<10	<10	<10	n.a.
V	ppm	27	50	110	400	n.a.
W	ppm	<20	<20	28	<20	n.a.
Y	ppm	9	10	12	27	n.a.
Zn	ppm	17	21	24	112	n.a.
Zr	ppm	34	33	29	53	n.a.

%; weight %; n.a.: not analyzed; >: above than upper instrumental detection limit; <: below than lower instrumental detection limit.

ed as of supergene origin (Fig. 9), could be the result of oxidized Cu released from Mn oxides, though the amount of Cu available from the Mn oxides is very low, considering that Cu

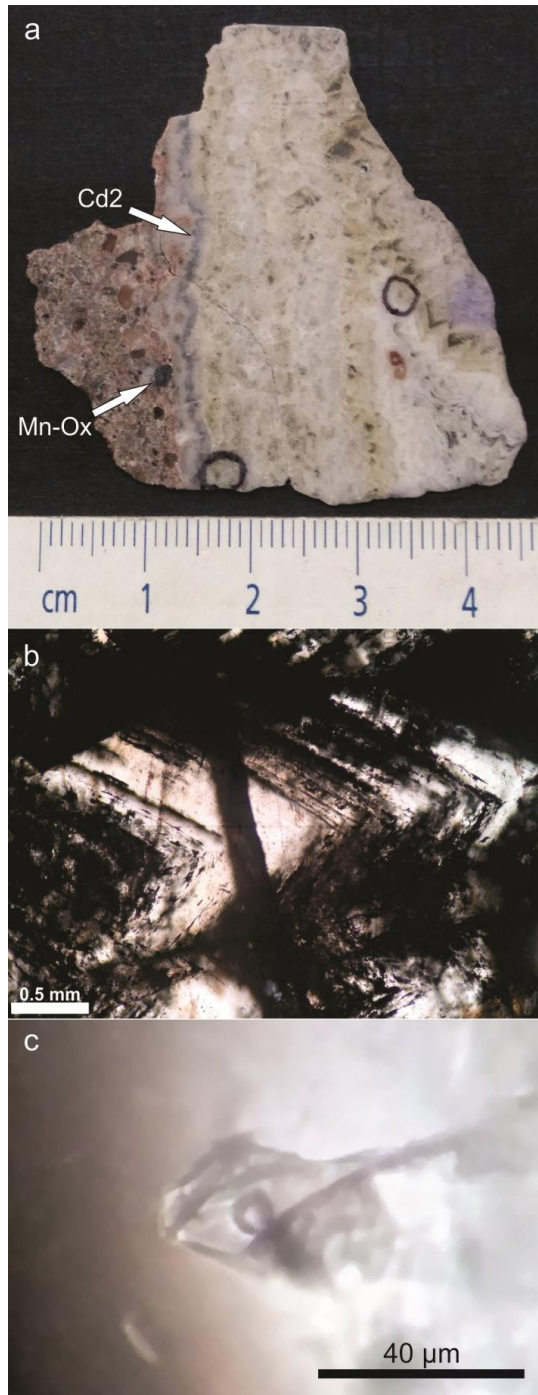


Figure 12. a. Large double polished slab evidencing infilling of calcite in an open fracture in arkose (to the left). Several generations of calcite are present in the image distinguished by alternating yellowish cream (fluorescent under long wave UV light) and whitish bands. The right side shows growth planes from the opposite side of the fracture (a microscopic view of growth planes is shown in more detail in figure 12 b). The left side of the image shows that chalcedony (Cd2) deposited prior to calcite on arkose. A cavity is filled with Mn oxides. Circled areas denote zones with some fluid inclusions chosen for microthermometric measurements. The light bluish tinge on the right border is ink staining. b. Rhombohedral growth planes in calcite outlined by irregular-shaped fluid inclusions (largely monophasic). Very scarce biphasic fluid inclusions may be found in these planes. c. Biphasic, isolated representative primary fluid inclusion at the border of a growth plane.

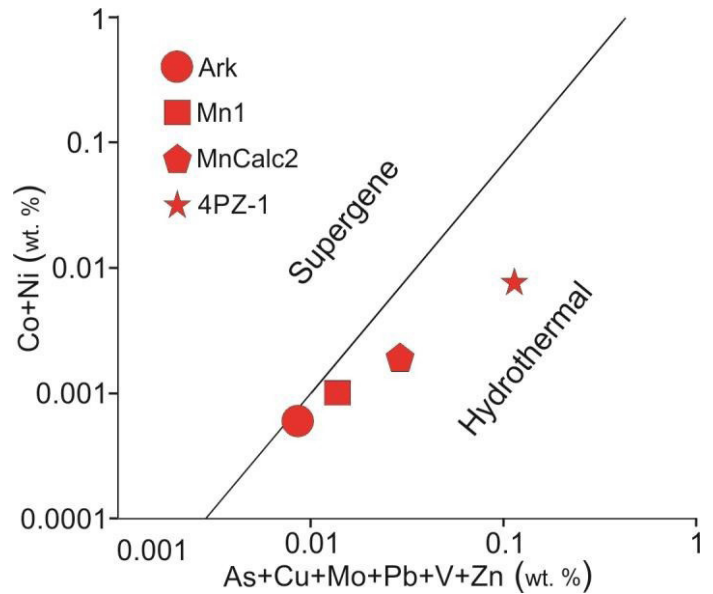


Figure 13. Polymetallic ratios of Nicholson (1992) as an approach to discriminate between hydrothermal and supergene (marine and freshwater) Mn oxides. The noticeable positive evolution trend between both discriminating group of elements has no other explanation that both groups of elements increase their content with increasing Mn contents (e.g., Cu is in negligible concentrations in the arkose as it also stands for Mn, but it reaches its maximum concentration in sample 4PZ-1, which is a highly pure Mn oxide concentrate). The observed trend is not inherited from geochemical natural processes but just as a response to the variable amounts of Mn oxide contained in each whole rock sample (except for Mn oxide hand-picked sample 4Pz-1). For a valid use of this graph we assumed that any elements from both groups are part of and genetically linked to the Mn oxides.

was not detected by EDS (below the detection limits); hence, it should not be discarded that that Cu could partially derive from the oxidation of sulfides from depth. The slightly anomalous values of Mo, V and Li detected only in sample MnCalc2 could imply that these elements are restricted to some areas of the Mn oxide - carbonate cemented breccia and are not of sedimentary origin; indeed, any of these elements showed anomalous values in the non-mineralized arkose sample (Ark). EDS analyses have shown that Sr is incorporated in variable amounts (~ 0.8 to 3.5 wt. %) in the formula of hollandite. The fact that the Mn oxide concentrate (sample 4Pz-1) displays the lowest Li content (28 ppm) and is comparable to those of the non-mineralized arkose (34 ppm) and sample Mn1 (32 ppm), suggests that the presence of anomalous Li (50 ppm) in sample MnCalc2 is not related to Mn oxide mineralization. The TI anomalous value in the Mn oxide concentrate (487 ppm) indicates that thallium could be likely adsorbed onto the Mn oxides (e.g., Crittenden et al. 1962, Wick et al. 2019, Garrido et al. 2020, Santos et al. 2021). The presence of primary TI traces might be found in several sulfides, particularly in pyrite (e.g., Xiong, 2007, George et al. 2019). If TI were related to

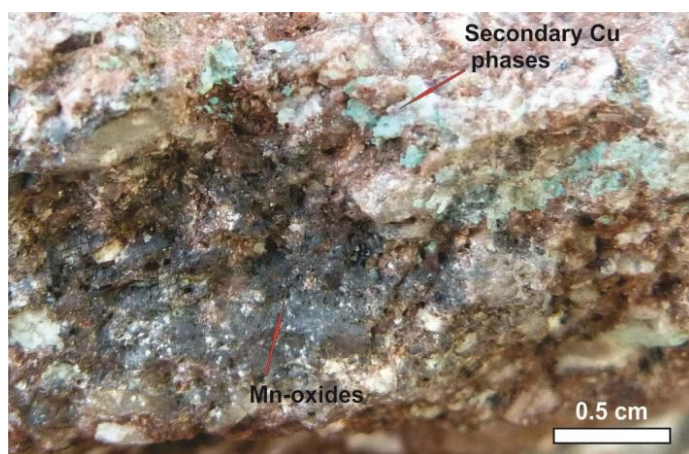


Figure 14. Coatings of a secondary Cu phase (probably chrysocolla) in arkose, associated with unidentified Mn oxides. Both were interpreted as mobilized products of supergene origin.

the potential presence of sulfides deeper below the oxidation zone, then the oxidation of sulfides could have released TI to be readily incorporated into hydrothermal Mn oxides.

Epithermal origin of mineralizing fluids

The extensional nature of the fault breccia is sustained by field evidence. Banded and druse infilling textures molded by different deposition pulses of Mn oxides, silica and calcite, are characteristic of the epithermal environment, particularly of calcite, which reveals five precipitation stages (Cc1 to Cc5), that were recognized based on different crystallographic habits and response to shortwave UV fluorescence. These five carbonate pulses likely represent gradual variations of fluid composition adjusted to decreasing fluid temperatures, which is commonly encountered in most hydrothermal environments. Whole-rock geochemistry data and the mineral chemistry composition of the Mn oxides support a hydrothermal origin for the precipitating fluids. The trapping temperatures of liquid-rich aqueous primary fluid inclusions within the temperature range of ~ 192 to ~ 255 °C and the common presence of monophasic fluid inclusions are also normal for epithermal fluids. Within and outside of the breccia zone, arkose is not hydrothermally altered, a fact that is attributed to very low water/rock ratios ($W \ll R$) and the strong silicification of the arkose matrix during the diagenetic stage that could have restricted fluid-rock interaction. Scarce Mn oxides associated to secondary Cu species might be found beyond the boundaries of the fault breccia, as products of supergene remobilization in the oxidation zone. These secondary Mn oxides are scarcely present in the quarry as spotty, sooty aggregates, lacking visible links with the fault breccia structure.

Metallogenetic considerations

Regardless of what is indicated by the Mn oxide geochemistry, the occurrence mode and crystallization sequence of Mn oxides, silica and carbonate phases, as well as the geochemical fingerprints, i.e. the TI and probably part of the Cu anomalies spatially restricted to the faulted-brecciated lineament, support a structurally controlled hydrothermal origin for the whole mineral assemblage.

The current degree of knowledge about the origin of the fluids involved in breccia cementation is poor. During this research work we were not able to find any evidence that could possibly relate the epithermal event with a particular magmatic or regional tectonic event. The most simplistic approach, mostly based on its nearest geographical proximity, would be to link the mineralizing occurrence with the magmatic event of the Permian-Triassic Magmatic Intracratonic Corridor (*Corredor Magmático Intracratónico Pérmico-Triásico*) of La Pampa province (Chernicoff et al. 2019). This corridor (CMPT-LP, Fig. 1a) consists of Late Permian to Mid Triassic intrusive and extrusive granitoids (e.g., syenogranite, rhyolite, leucogranite, bostonite, trondjemite) with an intraplate (anorogenic) signature. Genetically linked to this magmatism, Pires (2011) identified low sulfidation epithermal occurrences along the southernmost central portion of this plutonic-volcanic corridor. However, we are aware that this interpretation might not be appropriate considering that the magmatic corridor is very distant from the Los Cuatro Pozos epithermal occurrence (more than 120 km to the S and SW). In view of the absence of reported magmatism in the surroundings and at subsurface, a plausible metallogenetic link could exist with hidden plutonic or hypabissal intrusives related to a local basinal rift-related tectonic regime.

CONCLUSIONS

Los Cuatro Pozos quarry exposes a silicified arkose of continental origin and of probable Permian-Triassic age. Textural evidence suggests that massive silicification could be of diagenetic origin. A NE (25°) vertical fault zone crosscuts the arkose outcrop producing discontinuous patches of crackle, mosaic and chaotic breccias ranging from ~ 5 to 10 m thick. The precipitation sequence of localized breccia cementation started with hollandite, followed by quartz (early chalcedony and then idiomorphic quartz) and several generations of calcite with sporadic and negligible depositions of a second generation of hollandite, chalcedony and quartz prior to the third carbonate generation. Alternating bands of fluorescent with

non-fluorescent calcite (Cc1 to Cc4) and the modification of the crystallographic habit of calcite (Cc1 to Cc4= rhombohedral and Cc5= escalenohedral) evidence shifting fluid conditions during deposition. Geochemical tracers allowed interpreting a hydrothermal origin for the fluids. Banded and crystal lining druse textures characterize an epithermal environment in which fluid inclusion homogenization temperatures in calcite range from ~ 192 to 255 °C. The anomalous values of Sr are related to Sr-bearing hollandite. The anomalous concentration of Tl is intimately related to Mn oxides as it occurs with Cu as adsorbed elements. Both Cu and Tl might suggest the existence of sourcing sulfides at depth.

If the clastic sedimentary rocks would be truly of Permian-Triassic age, then faulting, brecciation and epithermal activity could be of Late Permian-Triassic age. Given the absence of outcropping or subsurface magmatic events in the vicinities of the Los Cuatro Pozos quarry, the extension-related, anorogenic Permian -Triassic Intracratonic Magmatic Corridor of La Pampa province could be considered as a potential source of mineralizing fluids, but it has a very remote location to be feasible. More likely, local rift-related basin tectonics could relate epithermal fluids with hidden, deeper seated intrusives.

ACKNOWLEDGEMENTS

We acknowledge Minería y Servicios S.A. for granting the access to the quarry, supporting field work and financing geochemical analyses, and for their authorization to publish data of their property. The project was supported with the financial aid of the Secretaría de Ciencia y Tecnología de la Universidad Nacional de Córdoba (grant Consolidar tipo 1 - 2018 - Res. 191/21 and 2022-155-E-UNC-SECYT#ACTIP). Maximiliano Medina from the LABGEO (CONICET-UNC) is acknowledged for the preparation of finely polished thick sections. Constructive criticisms of two anonymous reviewers helped significantly to improve this research work.

REFERENCES

Chernicoff, C.J. and Zappettini, E.O. 2005a. Evidencias de una cuenca de pull apart neopaleozoica en el sudeste de la provincia de San Luis, Argentina: extensión austral de la cuenca de Paganzo. 16° Congreso Geológico Argentino, Actas 1: 471-476, La Plata.

Chernicoff, C.J. and Zappettini, E.O. 2005b. Identification of the southernmost Paganzo basin deposits (Upper Paleozoic red beds) in south-central Argentina. Gondwana 12 Conference, Actas: 102, Mendoza.

Chernicoff, C.J. and Zappettini, E.O. 2007. La cuenca neopaleozoica de

Arizona, sudeste de San Luis, Argentina: prolongación austral de la cuenca de Paganzo. Comunicación, Revista de la Asociación Geológica Argentina 62(2): 321- 324.

Chernicoff, C.J., Zappettini, E.O., Santos, J.O and McNaughton, N. 2019. El Corredor Magmático Intracratónico Pérmico-Triásico de la provincia de La Pampa, Argentina: nuevas edades U-Pb SHRIMP, composición isotópica de Hf e implicancias geodinámicas. Revista Mexicana de Ciencias Geológicas 36(1): 13-26.

Costa, C., Ortiz Suárez, A., Miró, R., Chiesa, J., Gardini, C., Carugno Durán, A., Ojeda, G., Guerstein, P., Tognelli, G., Morla, P. and Strasser, E. 1999. Hoja Geológica 3366-IV Villa Mercedes. Provincias de San Luis y Córdoba. Programa Nacional de Cartas Geológicas de la República Argentina. Servicio Geológico Minero Argentino. Instituto de Geología y Recursos Minerales. 103 p., Buenos Aires.

Crittenden, M.D., Cuttitta, F., Rose Jr., H.J. and Fleischer, M. 1962. Studies on manganese oxide minerals VI. Thallium in some manganese oxides. The American Mineralogist 47: 1461-1467.

De Elorriaga, E.E. and Tullio, J.O. 1998. Estructuras del subsuelo y su influencia en la morfología en el norte de la provincia de La Pampa. 10° Congreso Latinoamericano de Geología y 6° Congreso Nacional de Geología Económica, Actas 3: 499-506, Buenos Aires.

Garrido, F., García-Guinea, J., Lopez-Arce, P., Voegelin, A., Göttlicher, J., Mangold, S. and Almendros, G. 2020. Thallium and co-genetic trace elements in hydrothermal Fe-Mn deposits of Central Spain. Science of the Total Environment 717: 137162.

George, L.L., Biagioni, C., Lepore, G.O., Lacalamita, M., Agrosi, G., Capitani, G.C., Bonaccorsi, E. and d'Acapito, F. 2019. The speciation of thallium in (Tl, Sb, As)-rich pyrite. Ore Geology Reviews 107: 364-380.

González Díaz, E.F. 1981. Geomorfología. In: Irigoyen, M. (ed.), Geología y recursos naturales de la provincia de San Luis, 8° Congreso Geológico Argentino, Relatorio: 193-264, San Luis.

Kostadinoff, J., Gregori, D., Raniolo, A., López, V. and Strazzere, L. 2006. Configuración geológica-geofísica del sector sur de la provincia de San Luis. Revista de la Asociación Geológica Argentina 61 (2): 279-285.

Laboratorio de Estructuras 2016. Análisis granulométrico, Norma IRAM 1505. Resistencia a la fragmentación usando la Máquina de Los Ángeles, Norma IRAM 1532. Informe de laboratorio, Departamento de Estructuras, FCEfYn, Universidad Nacional de Córdoba (unpublished), 2 p.

Laboratorio de Estructuras 2021. Análisis granulométrico, Norma IRAM 1505. Polvo adherido en agregados, Norma VN-E.68-75. Determinación de índice de lajosidad, IRAM 1687-1, Determinación del índice de elongación, IRAM 1687-2. Resistencia al desgaste usando la Máquina de Los Ángeles, Norma IRAM 1532. Informe de laboratorio, Departamento de Estructuras, FCEfYn, Universidad Nacional de Córdoba (unpublished), 3 p.

Linares, E., Llambías, E.J. and Latorre, C.O. 1980. Geología de la Provincia de La Pampa, República Argentina y geocronología de sus rocas metamórficas y eruptivas. Revista de la Asociación Geológica Argen-

- tina 35: 87-146.
- Nicholson, K. 1992. Contrasting mineralogical-geochemical signatures of manganese oxides: Guides to Metallogenesis. *Economic Geology* 87: 1253-1264.
- Párica, P.D. 1986. Petrología y geocronología del sector central de la Sierra de Lonco Vaca, La Pampa. *Revista de la Asociación Geológica Argentina* 41: 270-289.
- Pires, M.A. 2011. Provincia de La Pampa. Identificación y análisis de áreas metalíferas. Consejo Federal de Inversiones. Informe Final (unpublished), 126 p. and appendix, La Pampa.
- Romero, S.A. 1960. Yacimiento "estratégico" de "Los Cuatro Pozos" en el ángulo sudeste de San Luis. Informe técnico N° 125 (unpublished), Dirección Nacional de Vialidad, Buenos Aires.
- Salso, J.H. 1966. La Cuenca de Macachín, provincia de La Pampa. Nota preliminar. *Revista de la Asociación Geológica Argentina* 21: 107-117.
- Santos, J.L.O., Bueno, G.M.G., Flores, E.L.M., Leite, O.D., Janoni, C.R., Carvalhoe, L.G. and dos Santos, A.M.P. 2021. Thallium Associated with Manganese Ore Tailings in a Deactivated Mine in the Western Region of Bahia, Brazil. *Brazilian Chemical Society* 32 (5): 1120-1130. <https://dx.doi.org/10.21577/0103-5053.20210014>
- Viñas, N.A. 2005. Características geológicas del yacimiento de Cuatro Pozos, provincia de San Luis. Michelotti e Hijos S.R.L. (unpublished), 9 p, La Calera, Córdoba.
- Warr, L.N. 2021. IMA–CNMNC approved mineral symbols. *Mineralogical Magazine* 85: 291–320. doi:10.1180/mgm.2021.43
- Wick, S., Peña, J. and Voegelin, A. 2019. Thallium Sorption onto Manganese Oxides. *Environmental Science & Technology* 53: 13168–13178.
- Xiong, Y. 2007. Hydrothermal thallium mineralization up to 300 °C: A thermodynamic approach. *Ore Geology Reviews* 32: 291–313.